







## Open Archive Toulouse Archive Ouverte (OATAO)

OATAO is an open access repository that collects the work of Toulouse researchers and makes it freely available over the web where possible

This is an author's version published in: <http://oatao.univ-toulouse.fr/21897>

**Official URL:** <https://doi.org/10.1039/c8cp03312a>

### To cite this version:

Chiter, Fatah  and Bonnet, Marie-Laure  and Lacaze-Dufaure, Corinne  and Tang, Hao and Pébère, Nadine  *Corrosion protection of Al(111) by 8-hydroxyquinoline: a comprehensive DFT study.* (2018) *Physical Chemistry Chemical Physics*, 20 (33). 21474-21486. ISSN 1463-9076

Any correspondence concerning this service should be sent to the repository administrator: [tech-oatao@listes-diff.inp-toulouse.fr](mailto:tech-oatao@listes-diff.inp-toulouse.fr)

# Corrosion protection of Al(111) by 8-hydroxyquinoline: a comprehensive DFT study†

Fatah Chiter,<sup>ab</sup> Marie Laure Bonnet,<sup>a</sup> Corinne Lacaze Dufaure,<sup>id</sup>\*<sup>a</sup> Hao Tang<sup>b</sup> and Nadine Pèbère<sup>a</sup>

8-Hydroxyquinoline (8HQ) is a new green corrosion inhibitor. DFT-D calculations are performed to investigate the adsorption of 8HQ and derivatives on the Al(111) surface from low to high coverage. From  $\theta = 0.20$  to 0.66, the adsorption energies are 1.12, 2.41, 1.66 and  $-3.44$  eV per molecule for 8HQ, and its tautomer, its hydrogenated and its dehydrogenated species, independently of the coverage. In contrast, the geometry of the adsorbates changes between coverage up to 0.66 and the full monolayer ( $\theta = 1$ ). The creation of a dipole at the molecule/metal interface reduces the work function of aluminum. To further evaluate the modification of the reactivity of the surface, adsorption of  $O_2$  on the Al(111) surface covered by the organic layer is investigated.  $O_2$  dissociation takes place for  $\theta = 0.66$ . When the Al surface is fully covered ( $\theta = 1$ ), the reduction of  $O_2$  and the oxidation of Al atoms do not occur.

DOI: 10.1039/c8cp03312a

## 1 Introduction

The high toxicity and carcinogenic risks associated with chromates, used as corrosion inhibitors, have imposed restrictions on their use in industrial applications and their substitution by new environmentally friendly inhibitors. Among the numerous substances proposed to replace chromates, some friendly organic molecules have been identified<sup>1–3</sup> and experimental work has shown that 8-hydroxyquinoline (8HQ, with a chemical formula  $C_9H_7NO$  and presented in Fig. 1) is one of the most promising corrosion inhibitors of aluminum and aluminum alloys.<sup>4–14</sup>

Electrochemical studies performed on pure aluminum in neutral and acidic chloride solutions<sup>4,5</sup> or on aluminum alloys in acidic and alkaline solutions<sup>5–7</sup> showed that the presence of 8HQ in the electrolyte prevents the adsorption of aggressive ions on the Al surface oxide layer and limits the dissolution of the aluminum oxide layer. In addition, Yaro *et al.*<sup>8</sup> and Soliman<sup>9</sup> showed a decrease of the corrosion rate of aluminum alloys in an acidic medium with the increase of 8HQ concentration. Other work reported that 8HQ doped sol-gel coatings improve the corrosion resistance of the 2024 aluminum alloy.<sup>10,12</sup> More recently, Balaskas *et al.*<sup>13</sup> investigated by electrochemical methods the efficiency of 2-mercaptobenzothiazole (2-MBT), 8HQ and benzotriazole (BTAH) as corrosion inhibitors of 2024 aluminum alloy and concluded that 2-MBT is the most

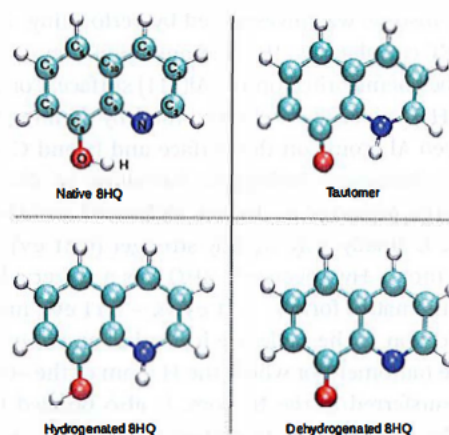


Fig. 1 Native 8HQ molecule ( $\chi$ ), and tautomer ( $\tau$ ), hydrogenated ( $\eta$ ) and dehydrogenated ( $\delta$ ) species.

efficient inhibitor and it is the only one that decreases anodic and cathodic reactions. Mixtures of inhibitors are also frequently used. Marcelin and Pèbère<sup>14</sup> confirmed that 8-HQ and BTAH are two effective corrosion inhibitors of AA2024. From local electrochemical impedance measurements, they demonstrated a synergistic effect between the two molecules and concluded that 8HQ acts mainly on the aluminum matrix. The electrochemical experimental studies suggested that the inhibitive efficiency of 8HQ could be explained thanks to: (i) the adsorption of the molecule on the Al surface and its interaction with the substrate, (ii) the formation of insoluble chelating complexes (tris(8-hydroxyquinoline) aluminum,  $Al(8HQ)_3$ ) over the aluminum oxide layer and (iii) less adsorption of aggressive species (chloride ions) which can damage the aluminum

<sup>a</sup> CIRIMAT, Université de Toulouse, CNRS, INPT-ENSIACET 4, allée Emile Monso, BP 44362, 31030 Toulouse Cedex 4, France. E-mail: corinne.dufaure@ensiacet.fr

<sup>b</sup> CEMES, UPR CNRS 8011, 29 Rue Jeanne Marvig, 31055 Toulouse Cedex 4, France

† Electronic supplementary information (ESI) available. See DOI: 10.1039/c8cp03312a

oxide layer. However, little is known about the origin of the mechanisms at the atomic scale. To our knowledge, only few investigations are available on the adsorption of 8HQ or of the  $\text{Al}(\text{8HQ})_3$  complex on metallic surfaces. A combined density functional theory (DFT) and non-contact atomic force microscopy (nc-AFM) study concerned intermolecular interactions between 8HQ molecules in molecular assemblies on a Cu(111) surface.<sup>15</sup> The observations, acquired on Cu(111) and in specific conditions imposed by AFM analyses such as low density deposition conditions, are particularly precise. In addition, in that work, Zhang *et al.* reported DFT calculations of selected 'flat-lying' 8-hydroxyquinoline (8HQ) molecular assemblies on a Cu(111) substrate to validate their interpretation of the AFM images. The aim of our study is different as we wanted to investigate the adsorption of 8HQ species present in aqueous solutions and at different pH, on Al(111).

In addition, DFT investigations on  $\text{Al}(\text{8HQ})_3$  complexes on cobalt,<sup>16</sup> magnesium<sup>17</sup> and aluminum<sup>18,19</sup> surfaces have been reported. These latter studies focused mainly on the creation of a dipole at the  $\text{Al}(\text{8HQ})_3/\text{metal}$  interface.

In a previous study on the bonding of 8HQ and its derivatives on an Al(111) surface, we reported the main characteristics of the interaction mechanisms at low coverage.<sup>20</sup> The adsorption of the 8HQ molecule and its derivatives, tautomer, dehydrogenated and hydrogenated 8HQ species, which are present in the experimental medium according to the pH of the solution, on the Al(111) substrate was investigated by performing dispersion corrected DFT calculations. We demonstrated that all the 8HQ species can be chemisorbed on the Al(111) surface. For example, the native 8HQ molecule is chemisorbed by forming covalent bonds between Al atoms on the surface and N and C atoms of the molecule. However, during the formation of the covalent bonds, the 8HQ molecule is strongly deformed and the chemisorbed mode is finally only slightly stronger (0.21 eV) than the physisorbed mode. Hydrogenated 8HQ has a larger adsorption energy than the native form (-1.71 eV vs. -1.11 eV), mainly due to lower distortion of the molecule instead of an increase of the bonding. The tautomer, for which the H atom of the -OH group in 8HQ is transferred to the N atom, is also bonded to the Al surface by the O atom and the adsorption energy is stronger (-2.39 eV). Finally, the dehydrogenated 8HQ species has the strongest bonding with an adsorption energy of -3.45 eV. In all the cases, a strong contribution of the vdW forces at the molecule/metal interface in the adsorption mechanism is observed. But the orientation of the molecules with respect to the surface and the stability of the molecular layer depend on the surface coverage and these characteristics are assumed to influence the inhibitor efficiency. At high surface coverage, intermolecular interactions could stabilize specific adsorption modes. A. Kokalj<sup>21</sup> showed for instance, that a properly orientated adsorption structure of BTAH on the Cu(111) surface modifies significantly the electronic properties of the metallic surface (a decrease of the work function). The efficiency of BTAH on copper was also studied by Y. Jiang *et al.*<sup>22</sup> and was attributed to the physisorption of the molecules and the formation of an intermolecular H-bonding network, which resulted in a thin and protective film

on the surface. Derivatives of BTAH were also investigated and it was shown that the chemisorption of the dehydrogenated radical is the most stable at low coverage and in contrast, the formation of a full layer occurs in the form of a physisorbed layer or an organometallic layer.<sup>23</sup> It was also observed that the adsorption energy of the BTAH molecule on the  $\text{Cu}_2\text{O}(111)$  surface increases with the surface coverage<sup>24</sup> and that the molecules are strongly adsorbed forming covalent bonds with the Cu atoms and hydrogen bonds with the surface O atoms. Recently, DFT calculations including dispersive corrections showed that structures of dimers and chains of BTA molecules are the most stable topologies on Cu(111) at all coverages.<sup>25</sup>

Others examples of the influence of the surface coverage on the adsorption properties of organic layers on metals are given in the literature. For instance, the adsorption of glycine<sup>26</sup> and carboxylic acids (CA)<sup>27</sup> on zinc surfaces was investigated from low to high coverage. For glycine, dissociative adsorption to form a glycinate species is favorable independently of the surface coverage. However, at low coverage, the most stable configuration is parallel to the surface whereas at higher coverage an epitaxial glycinate monolayer is organized on the Zn-ZnO(0001) surface.<sup>26</sup> For the carboxylic acids, the bridging adsorption mode and self-assembled monolayer formation are attributed to van der Waals forces through lateral interactions of the carbon chains of the molecules.<sup>27</sup>

In the present work, the formation of layers by 8HQ and derivatives (presented in Fig. 1) on Al(111) is investigated and the influence of the coverage of the Al(111) surface on the adsorption topologies and adsorption energies of the organic molecules is presented and understood. Charge transfers due to the adsorption process are calculated and give evidence for covalent bonding. In addition, van der Waals interactions also contribute to the formation of the molecular layer on the Al surface. The interface dipole created at the molecule/metal interface and the Al(111) work function change are determined and the relationship between these two quantities is highlighted. Finally, the modification of the reactivity of the covered Al(111) surface towards the oxygen molecule is evaluated in order to link the computed results with the experimental inhibition efficiency.

## 2 Computational models and details

All calculations were performed in the framework of Density Functional Theory (DFT) using the Vienna Ab initio Simulation Package<sup>28-30</sup> (VASP) and the Projector Augmented Wave (PAW) method,<sup>31,32</sup> taking into account the spin polarization. The Generalized Gradient Approximation (GGA) of Perdew-Burke-Ernzerhof<sup>33,34</sup> (PBE) functional was chosen for the exchange-correlation term. Convergence with respect to cutoff energy  $E_{\text{cut}}$ , Methfessel-Paxton<sup>35</sup> smearing  $\sigma$  and the size of the Monkhorst-Pack<sup>36</sup> mesh of  $k$ -points was carefully checked in order to have the same energy precision in all calculations (less than 1 meV per atom). Values of  $E_{\text{cut}} = 450$  eV and  $\sigma = 0.1$  eV were used. For the studies of molecular oxygen dissociation,

tests were performed with a higher  $E_{\text{cut}}$  value (900 eV) and led to the same results.

The Al substrate was described by an asymmetric monoclinic slab of 4 atomic layers. Atoms of the two bottom layers were kept at their position in the bulk during all computations. The atoms of the two top layers of the slab and of the adsorbed molecules were optimized. Atomic positions were relaxed with the conjugate gradient algorithm until forces on each moving atom were less than  $0.02 \text{ eV \AA}^{-1}$ . The vacuum region was set at  $18 \text{ \AA}$  (equivalent to 8 atomic layers thick) to minimize the interactions in the  $z$  direction between periodic images of the molecule/substrate system. The molecules were adsorbed on the top layer of the slab with different surface coverages. The lowest coverage ( $\theta = 0.2$ ) was selected to minimize the interaction between the adsorbed molecule and its periodic images on a  $(5 \times 6)$  array (an Al surface area of  $212 \text{ \AA}^2$ ). The lateral dimension of the supercell was then successively

decreased with one 8HQ molecule per unit cell to mimic the increase of the surface coverage. The surface coverage  $\theta = 1$  was reached when the Al(111) surface was fully covered by the 8HQ molecules or derivatives (Fig. 2,  $\theta = 1$ ). Five supercells containing 30, 20, 12, 9 and 6 aluminum surface atoms were used to simulate  $\theta = 0.20, 0.33, 0.5, 0.66$  and  $1$ , respectively. The  $k$ -point grid for the reciprocal Brillouin zone sampling was increased accordingly (see Table 1).

For the study of the dissociation of the  $\text{O}_2$  molecule on the Al(111) surface covered by organic layers ( $\theta = 0.66$  and  $\theta = 1$ ), a  $(6 \times 6)$  array was chosen for the metallic slab (144 atoms) with a sampling of  $(3 \times 3 \times 1)$   $k$ -points in the Brillouin zone.

van der Waals interactions were included according to the DFT-D2 method<sup>37</sup> implemented in VASP. As in our previous work on the adsorption at low coverage,<sup>20</sup> only interactions at the molecule/aluminum interface and between molecules in

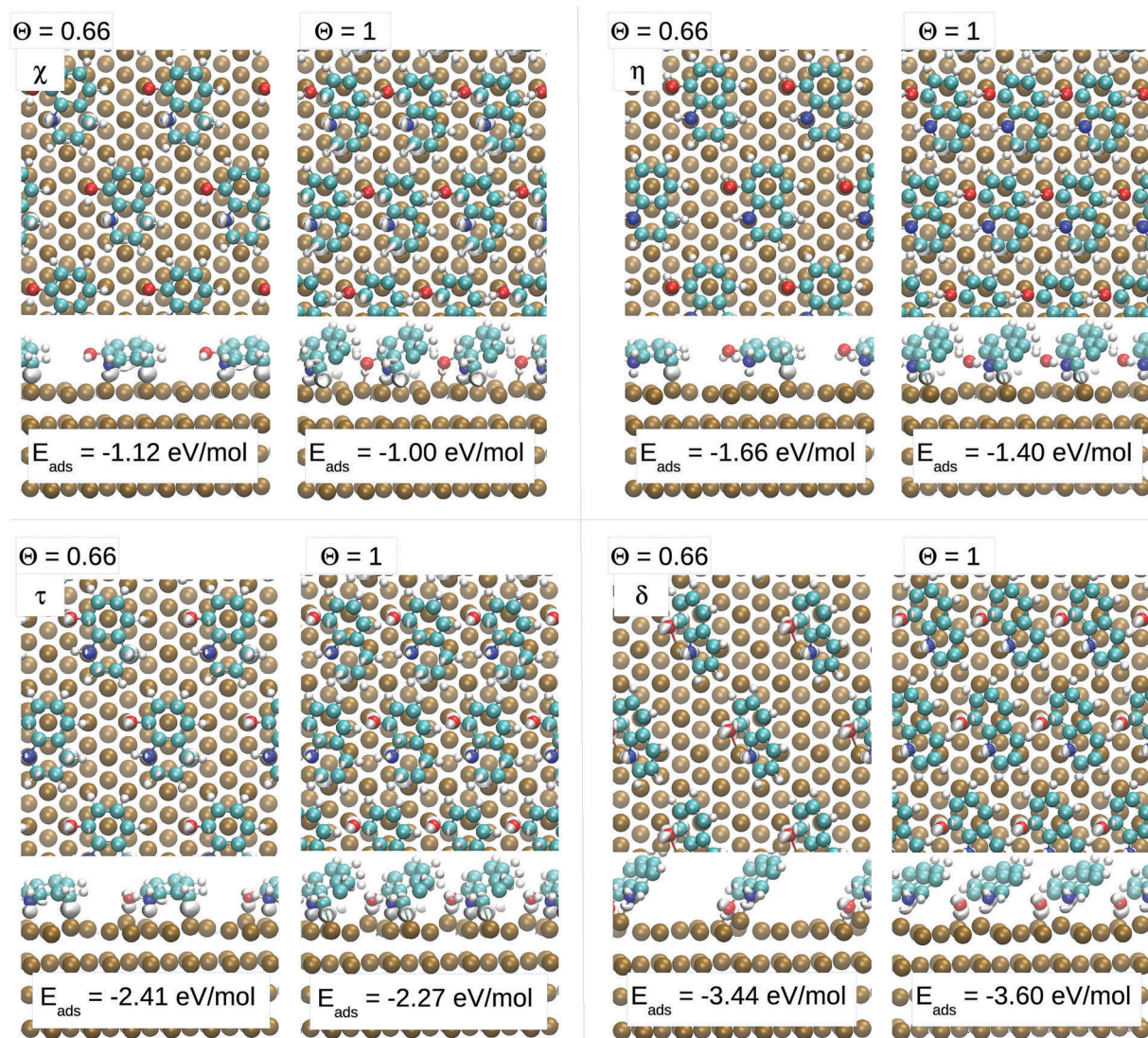


Fig. 2 Adsorption topologies and electronic density variation ( $\Delta\rho$ ) at two coverages ( $\theta = 0.66$  and  $\theta = 1$ ). The 8HQ molecule ( $\chi$ ); and the tautomer ( $\tau$ ). Top: Top view; and bottom: side view.

**Table 1** Grid of  $k$  points for molecule/slab calculations according to the coverage  $\theta$ 

Coverage $\theta$	0.20	0.33	0.5	0.66	1
Number of atoms in the surface	30	20	12	9	6
Number of atoms in the unit cell	120	80	48	36	24
Surface area ( $\text{\AA}^2$ )	212	141	85	64	42
$k$ Points	$3 \times 3 \times 1$	$3 \times 3 \times 1$	$5 \times 5 \times 1$	$5 \times 5 \times 1$	$7 \times 7 \times 1$

the organic layer were considered. The total energy was therefore calculated for the (slab + molecules) system by:

$$E_{\text{tot}}^{\text{DFT-D}} = E_{\text{tot}}^{\text{DFT}} + E_{\text{slab/mol}}^{\text{vdW}} + E_{\text{mol/mol}}^{\text{vdW}} \quad (1)$$

with  $E_{\text{slab/mol}}^{\text{vdW}}$  the vdW interactions at the aluminum/molecule interface and  $E_{\text{mol/mol}}^{\text{vdW}}$  the vdW interactions between the molecules.

From the total energies, two energetic features were calculated to quantify the molecule/surface interactions. The first one,  $E_{\text{ads}}$ , characterized the simultaneous adsorption of all the molecules from their free state. The adsorption energy on the Al(111) surface was thus calculated as:

$$E_{\text{ads}} = E_{\text{slab+mol}} - E_{\text{slab/opt}} - E_{\text{mol/opt}} \quad (2)$$

where  $E_{\text{slab+mol}}$  is the total energy of the system with the molecule adsorbed on the Al(111) surface,  $E_{\text{slab/opt}}$  is the energy of the bare relaxed Al(111) slab calculated without dispersive corrections and  $E_{\text{mol/opt}}$  is the energy of the free molecule optimized in vacuum.

The binding energy,  $E_{\text{bind}}$ , characterized the strength of the bonding at the molecule/aluminum interface without taking into account energetic trends for the deformation of the substrate and the adsorbate induced by the formation of the layer on Al(111). The binding energy was then defined as:

$$E_{\text{bind}} = E_{\text{slab+mol}} - E_{\text{slab/sp}} - E_{\text{mol-layer/sp}} \quad (3)$$

where  $E_{\text{slab+mol}}$  is the total energy of the system with the molecule adsorbed on the Al(111) surface and  $E_{\text{slab/sp}}$  and  $E_{\text{mol-layer/sp}}$  are the total energies of the isolated slab and isolated deformed molecular layer at their geometry after adsorption, respectively.

Therefore, the deformation energies of the substrate  $E_{\text{slab}}^{\text{deform}}$  and of the molecule  $E_{\text{mol}}^{\text{deform}}$  during the adsorption process were evaluated. The substrate deformation energy  $E_{\text{slab}}^{\text{deform}}$  was calculated as:

$$E_{\text{slab}}^{\text{deform}} = E_{\text{slab/sp}} - E_{\text{slab/opt}} \quad (4)$$

where  $E_{\text{slab/sp}}$  and  $E_{\text{slab/opt}}$  are the total energy of the isolated slab at the geometry after adsorption and the total energy of the relaxed slab, respectively.

The molecule deformation energy  $E_{\text{mol}}^{\text{deform}}$  was determined as:

$$E_{\text{mol}}^{\text{deform}} = E_{\text{mol/sp}} - E_{\text{mol/opt}} \quad (5)$$

where  $E_{\text{mol/sp}}$  and  $E_{\text{mol/opt}}$  are the total energy of the isolated molecule at the geometry after adsorption (one molecule per unit cell) and of the optimized free molecule, respectively.

Finally, the interactions between molecules in the layer were evaluated from the calculation of the cohesive energy per molecule in the organic layer  $E_{\text{layer}}^{\text{coh}}$  by:

$$E_{\text{layer}}^{\text{coh}} = E_{\text{mol-layer/sp}} - E_{\text{mol/sp}} \quad (6)$$

where  $E_{\text{mol-layer/sp}}$  is the total energy of the isolated layer and  $E_{\text{mol/sp}}$  is the energy of the isolated molecule at the geometry after adsorption without interaction with the periodic images (large unit cell).

To quantify the electronic changes in the systems, the net charge variation ( $\Delta q_x$ ) was determined on each atom by:

$$\Delta q_x = q_x^{\text{ads}} - q_x^{\text{free}} \quad (7)$$

where  $q_x^{\text{free}}$  and  $q_x^{\text{ads}}$  are the charges on each atom  $x$  (Bader's population analysis on VASP charge densities<sup>38</sup>) of the molecule and the slab before (optimized geometries of the free systems) and after adsorption. The total molecular charge variation  $\Delta Q_{\text{mol}}$  was calculated as:

$$\Delta Q_{\text{mol}} = Q_{\text{mol}}^{\text{ads}} - Q_{\text{mol}}^{\text{free}} \quad (8)$$

To clearly observe the charge transfer, the electron density variation  $\Delta\rho$  was plotted:

$$\Delta\rho = \rho_{\text{slab+mol}} - (\rho_{\text{slab/sp}} + \rho_{\text{mol-layer/sp}}) \quad (9)$$

where  $\rho_{\text{slab+mol}}$  is the electron density distribution on the optimized system, and  $\rho_{\text{slab/sp}}$  and  $\rho_{\text{mol-layer/sp}}$  are the electron density distributions on the substrate and molecular layer at the geometry after adsorption, respectively.

## 3 Results and discussion

### 3.1 Adsorption of 8HQ species on the Al(111) surface

We took into account experimental results presented in the literature with bulk 8HQ or in polar solvent. 8HQ molecules are associated as dimer molecules (with hydrogen bonds between two monomers) in the bulk 8HQ crystal.<sup>39</sup> When the crystal in powder is introduced in a polar solvent, which is the case when studying corrosion inhibitors in aqueous solution, the dimer molecules are dissociated and 8HQ molecules (monomers) are the main species in the solution.<sup>40-42</sup> We thus studied the interaction of 8HQ monomers with the Al(111) surface. Preliminary calculations were also performed on the adsorption of the 8HQ dimer on the Al(111) surface and results are presented in the ESI.† To mimic the different chemical forms of the molecule present in aqueous solution at different pH, we looked at the  $pK_a$  values of the 8HQ molecule. Many organic molecules can gain and/or lose a proton in aqueous solutions by reacting with water molecules. These phenomena are dependent on the pH of the solution. The  $pK_a$  of a molecule gives information on its ability to be protonated or deprotonated at a certain pH and, for a given molecule, two  $pK_a$  values indicate the presence of two different functional groups that can be protonated or deprotonated. The  $pK_a$  values of the 8HQ molecule are 5.13 and 9.89.<sup>40</sup> In neutral solution,

the native 8HQ molecule ( $\chi$ ) and its tautomer ( $\tau$ ) (Fig. 1) coexist. At low pH (pH < 5.13), the 8HQ molecule is protonated, whereas at high pH (pH > 9.89) it is deprotonated. The modeling of charged species is not trivial because periodic boundary calculations impose the use of charge neutrality in the system. Therefore, the adsorption of the hydrogenated ( $\eta$ ) and dehydrogenated ( $\delta$ ) species, which are radicals, was studied to simulate the adsorption of the charged species of 8HQ at low and high pH. This assumption is usually done in periodic calculations.<sup>21,43</sup> For the different surface coverages, several initial configurations (including high symmetry adsorption sites on the surface unit cell) for the adsorption of the 8HQ molecule and its derivatives on the Al(111) surface were considered. The reactive sites of the molecules (O, N, ortho C2 and para C4 sites) were initially positioned on the different Al(111) surface sites (top, bridge, hollow-fcc and hollow-hcp sites).

In the present paper, only the most stable optimized configuration for each species and at each coverage is presented. The adsorption energetics (Fig. 3–5) are analyzed by taking into account the simultaneous elementary steps of the adsorption mechanism for the formation of an organic layer: (i) the molecule/metal interactions ( $E_{\text{bind}}$ ), (ii) the deformation of the molecules due to the adsorption modes ( $E_{\text{mol}}^{\text{deform}}$ ), (iii) the deformation of the metallic surface during the adsorption process ( $E_{\text{slab}}^{\text{deform}}$ ) and (iv) the interactions between the molecules in the layer ( $E_{\text{layer}}^{\text{coh}}$ ). In addition, the modifications in the interatomic distances as a function of  $\theta$  are summarized in Table 2.

**3.1.1 Adsorption geometries and energies for the 8HQ species as a function of the coverage ( $\theta$ ).** The adsorption of native 8HQ (labeled  $\chi$ ) and its derivatives ( $\tau$ ,  $\eta$  and  $\delta$ ) at low coverage ( $\theta = 0.20$ ) was previously described.<sup>20</sup> At this low coverage, the native 8HQ molecule is chemisorbed parallel to the aluminum surface with an adsorption energy of  $-1.11$  eV ( $\theta = 0.2$ ).<sup>20</sup> Covalent bonds are created between the N atom and the C4 atom of the molecule (numbering in Fig. 1) and atoms of the Al(111) surface. In the present work, results at higher surface coverages ( $\theta = 0.3$  to 1) are presented. By increasing progressively  $\theta$  to 0.3, 0.5 and 0.66, the conformation of the chemisorbed  $\chi$  molecules on the Al(111) surface does not change significantly and the molecules are always bonded to the Al(111) surface through covalent bonds formed by N and C4 atoms with surface Al atoms (see the adsorption configuration in Fig. 2 for  $\theta = 0.66$  and distances in Table 2). However, for the transition from  $\theta = 0.66$  to  $\theta = 1$ , due to the high density of adsorbed molecules on the surface, their parallel topology cannot be kept. For  $\theta = 1$ , the C4–Al bond does not exist any more ( $d_{\text{C4-Al}} = 3.684$  Å in Table 2; instead, a new C2–Al bond is created,  $d_{\text{C2-Al}} = 2.178$  Å) and the electron density accumulation ( $\Delta\rho$  in Fig. 2) indicates covalent bonding. In addition, the oxygen atom of the hydroxyl group is situated at  $2.073$  Å exactly above an Al atom in the surface.

In the case of the tautomer ( $\tau$ ), from  $\theta = 0.2$  to 0.66, three bonds (O–Al, N–Al and C4–Al) ensure strong bonding with the Al(111) surface. The interatomic distances reported in Table 2 ( $d_{\text{O-Al}} = 1.844 \pm 0.006$  Å,  $d_{\text{N-Al}} = 2.222 \pm 0.005$  Å and  $d_{\text{C4-Al}} = 2.185 \pm 0.004$  Å) underline the strong bonding of the tautomer. Here again, for  $\theta = 1$ , a significant geometrical change similar to

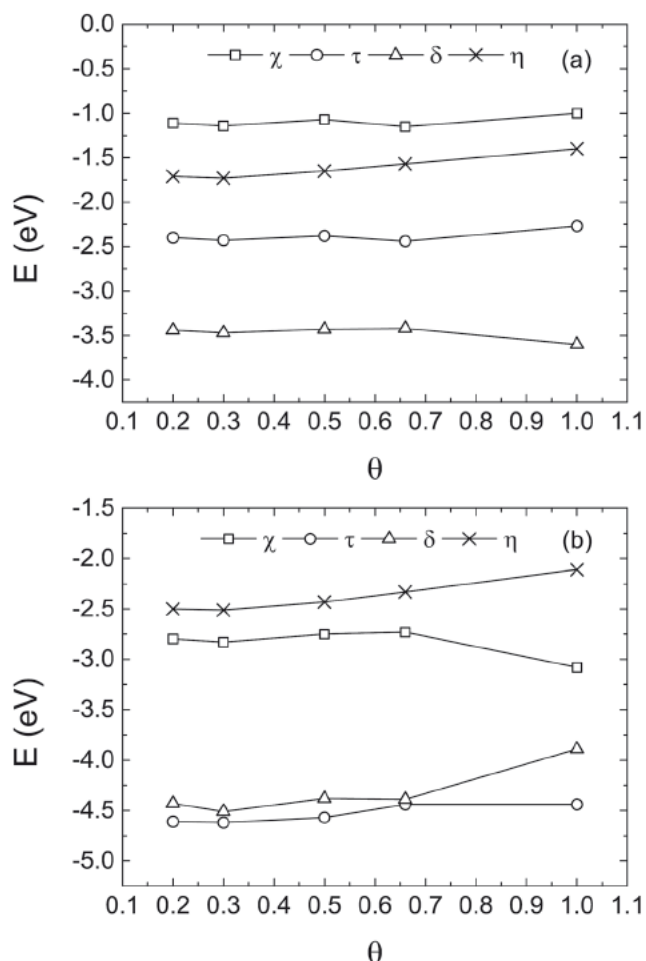


Fig. 3 Adsorption and binding energies of the molecules on the Al(111) surface versus the coverage  $\theta$ . The 8HQ molecule ( $\chi$ ); the tautomer ( $\tau$ ); dehydrogenated 8HQ ( $\delta$ ); and hydrogenated 8HQ ( $\eta$ ). (a) adsorption energies; and (b) binding energies.

that of native 8HQ is observed with again the replacement of the C4–Al bond by a C2–Al bond ( $d_{\text{C2-Al}} = 2.168$  Å and  $d_{\text{C4-Al}} = 3.707$  Å). On the contrary, the O–Al bond is kept ( $d_{\text{O-Al}} = 1.814$  Å).

For the hydrogenated form ( $\eta$ ), the geometrical evolution of the adsorbed molecules as a function of the coverage is very similar to that of native 8HQ in spite of the presence of the H atoms on the O and N atoms: from  $\theta = 0.2$  to 0.66, the species is chemisorbed on the Al(111) surface through two covalent bonds, *i.e.* N–Al ( $d_{\text{N-Al}} = 2.315 \pm 0.004$  Å) and C4–Al ( $d_{\text{C4-Al}} = 2.180 \pm 0.004$  Å). For  $\theta = 1$ , the C4–Al bond is deleted ( $d_{\text{C4-Al}} = 3.808$  Å) and the C2–Al bond ( $d_{\text{C2-Al}} = 2.219$  Å) is established.

The influence of the surface coverage on the adsorption of the dehydrogenated form ( $\delta$ ) is totally different to those obtained for the three previous molecule derivatives. For the dehydrogenated species, both the O and N atoms remain bonded to the surface from  $\theta = 0.2$  until  $\theta = 1$ . The geometrical modification with the increase of the coverage is small in comparison to the changes of the adsorbed  $\chi$ ,  $\tau$  and  $\eta$  molecules going from  $\theta = 0.66$  to  $\theta = 1$ . The only noticeable change in the  $\delta$  topology is a modification of the adsorption position of the

**Table 2** Distances in Å between the Al surface atoms and the atoms of the 8HQ molecule and its derivatives after adsorption for different coverages  $\theta$

Coverage	O Al	N Al	C2 Al	C4 Al
<b>8HQ</b>				
$\theta$ 0.2	2.659	1.968	2.948	2.189
$\theta$ 0.3	2.701	1.967	2.957	2.191
$\theta$ 0.5	2.762	1.969	3.000	2.188
$\theta$ 0.66	2.745	1.966	2.905	2.184
$\theta$ 1	2.073	1.916	2.178	3.684
<b>Tautomer</b>				
$\theta$ 0.2	1.838	2.223	3.154	2.182
$\theta$ 0.3	1.841	2.224	3.153	2.187
$\theta$ 0.5	1.844	2.223	3.160	2.184
$\theta$ 0.66	1.852	2.217	3.146	2.189
$\theta$ 1	1.814	2.095	2.168	3.707
<b>Hydrogenated 8HQ</b>				
$\theta$ 0.2	3.021	2.314	3.281	2.176
$\theta$ 0.3	3.019	2.311	3.271	2.179
$\theta$ 0.5	3.026	2.311	3.279	2.176
$\theta$ 0.66	3.091	2.324	3.284	2.187
$\theta$ 1	2.263	2.198	2.219	3.808
<b>Dehydrogenated 8HQ</b>				
$\theta$ 0.2	1.914	2.048	3.373	4.710
$\theta$ 0.3	1.914	2.044	3.402	4.402
$\theta$ 0.5	1.907	2.050	3.421	4.929
$\theta$ 0.66	1.917	2.032	3.453	4.902
$\theta$ 1	1.822	2.119	3.510	4.492

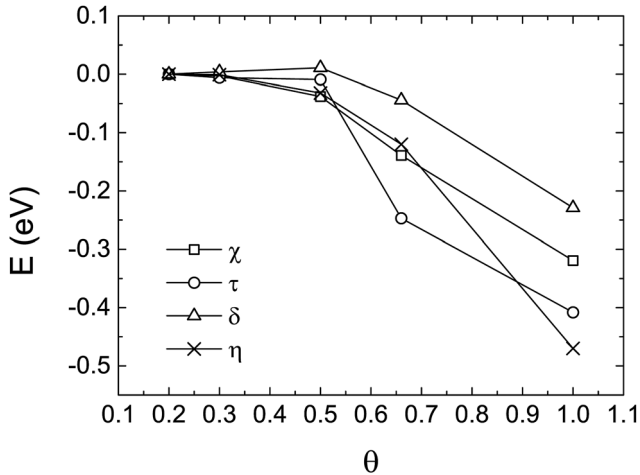


**Fig. 4** Cohesive energies in the layers for different coverages  $\theta$ : The 8HQ molecule ( $\chi$ ); the tautomer ( $\tau$ ); dehydrogenated 8HQ ( $\delta$ ); and hydrogenated 8HQ ( $\eta$ ).

O atom from a bridge site on the Al(111) surface for  $\theta = 0.2$  to  $0.66$  to a top site for  $\theta = 1$  (Fig. 2). For  $\theta = 1$ , the O, N, C2 and C4 atoms of the four molecules are located on top of Al atoms.

Fig. 3(a) presents the variation of the adsorption energy  $E_{\text{ads}}$  with the coverage  $\theta$  of the 8HQ molecule and its tautomer, hydrogenated and dehydrogenated forms on the Al(111) surface. Negative adsorption energies are obtained for all species and coverages, indicating the formation of a stable organic layer on Al(111). From  $\theta = 0.2$  to  $0.66$ , constant adsorption energies of  $-1.12 \pm 0.04$  eV for native 8HQ,  $-1.66 \pm 0.07$  eV for the

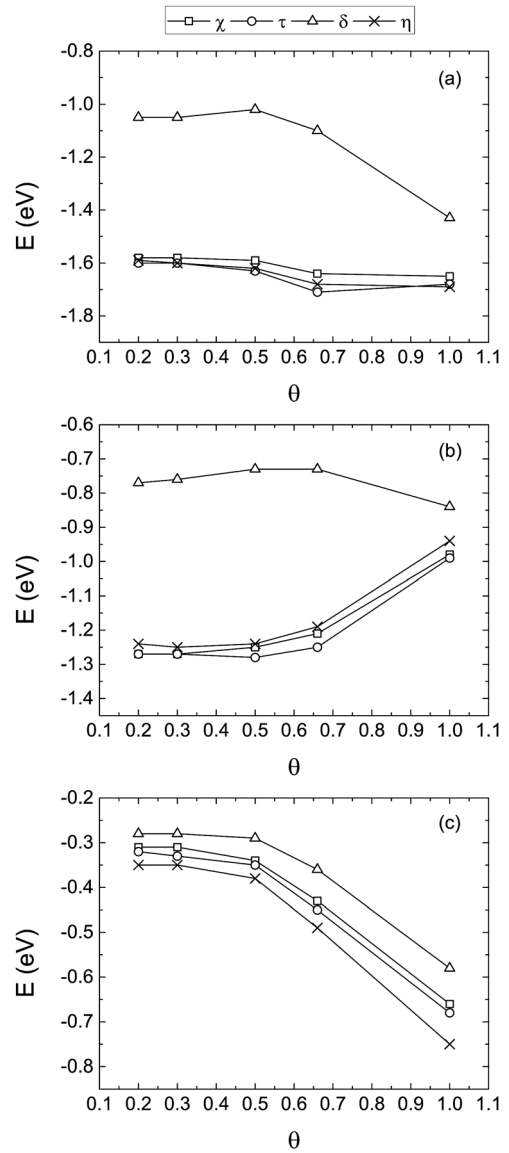


**Fig. 5** Contribution of the dispersion forces at different coverages  $\theta$  for the adsorption of the molecules on the Al(111) surface. The 8HQ molecule ( $\chi$ ); the tautomer ( $\tau$ ); dehydrogenated 8HQ ( $\delta$ ); and hydrogenated 8HQ ( $\eta$ ). (a) Total vdW energies, (b) vdW energies at the molecule/substrate interface, and (c) vdW energies in the organic layer.

hydrogenated molecule,  $-2.41 \pm 0.02$  eV for the tautomer, and  $-3.44 \pm 0.02$  eV for the dehydrogenated species are calculated. For  $\theta = 1$ , the native 8HQ, the hydrogenated, the tautomer and the dehydrogenated molecules have an adsorption energy of  $-1.00$  eV,  $-1.40$  eV,  $-2.27$  eV and  $-3.60$  eV, respectively. However the adsorption energy values includes not only the bonding of the molecule to the surface but also the deformation of the molecule and of the slab due to the adsorption process. The binding energy,  $E_{\text{bind}}$ , shown in Fig. 3(b), only quantifies the bonding at the molecule/metal interface without taking into account the energetic cost of the deformation of the slab and the deformation of molecules in the organic layer, and the interactions between molecules. Due to the covalent character

of the bonding, the binding energies (per molecule) are significantly larger (by about 0.5 eV for  $\eta$  up to more than 2 eV for  $\tau$ ) than the adsorption ones that are drastically reduced (in absolute value) by the positive (destabilizing) deformation energies. From  $\theta = 0.2$  to 0.66, the molecule deformation energies are strong with values of  $0.55 \pm 0.01$  eV ( $\delta$ ),  $0.71 \pm 0.03$  eV ( $\eta$ ),  $1.57 \pm 0.01$  eV ( $\chi$ ) and  $1.96 \pm 0.01$  eV ( $\tau$ ). At these coverages, the slab deformation energies when adsorbing  $\chi$ ,  $\tau$  and  $\eta$  are rather weak (about 0.13 eV for  $\chi$ , 0.10 eV for  $\eta$  and 0.25 eV for  $\tau$ ), whereas when  $\delta$  is adsorbed, the slab deformation energy reaches 0.45 eV.

As previously explained, in addition to the deformation energies, the adsorption energy takes also into account the interactions between the molecules in the organic layer. The cohesive energy  $E_{\text{layer}}^{\text{coh}}$  of the layers formed on the Al(111) surface at different coverages is shown in Fig. 4. The energies were calculated by only taking into account the interactions between the molecules in the layer and not the deformation of the molecules during the adsorption process (eqn (6)). The results show a change for  $\theta = 0.5$  to 1 with negative values of  $E_{\text{layer}}^{\text{coh}}$  that indicate stabilizing interactions between molecules. At low coverages, the molecules are not close enough to be interacting ( $E_{\text{layer}}^{\text{coh}} \approx 0$ ). At full coverage,  $E_{\text{layer}}^{\text{coh}}$ , that quantifies the interactions in the layer, represents 6% of the adsorption energy  $E_{\text{ads}}$  for the dehydrogenated species, 18% for the tautomer and up to 30% and 32% for the native 8HQ and the hydrogenated species.

To sum up all these energetic features, it can be written:

$$E_{\text{ads}} = E_{\text{bind}} + E_{\text{mol}}^{\text{deform}} + E_{\text{slab}}^{\text{deform}} + E_{\text{layer}}^{\text{coh}}$$

In this equation, it must be underlined that the molecule and slab deformation energies are unfavorable for a stable layer on the Al(111) surface, and in contrast, the molecule/surface binding energy and the intermolecular cohesion energy are the driving force of the adsorption process.

**3.1.2 van der Waals dispersive forces.** Only van der Waals interactions between the organic layer and the Al(111) surface and between the molecules in the layer were taken into account. Fig. 5(a) presents the total van der Waals energy in the systems. Fig. 5(b) and (c) show the variation of the vdW energies as a function of the coverage  $\theta$  at the molecule/substrate interface and between molecules in the layer, respectively. The native 8HQ molecule, the tautomer and the hydrogenated species show similar trends and this can be linked to comparable topology on the surface (topology parallel to the surface). For these three species, the total vdW energy decreases slightly with increasing coverage showing that the van der Waals interactions increase. The average value is  $-1.63 \pm 0.06$  eV. For the dehydrogenated molecules, the value is  $-1.06 \pm 0.04$  eV from  $\theta = 0.2$  to 0.66 and  $-1.43$  eV at full coverage ( $\theta = 1$ ). From  $\theta = 0.2$  to 0.66, the vdW energy at the molecule/substrate interface is  $-1.24 \pm 0.05$  eV for native 8HQ, the tautomer and the hydrogenated species and  $-0.96 \pm 0.03$  eV for  $\theta = 1$  (Fig. 5(b)). The decrease of the interactions (increase of the van der Waals energy) can be attributed to the topological

change occurring at full coverage, where the molecules become tilted on the Al(111) surface. Thus, the contact between the molecules and the substrate is reduced and vdW interactions at the interface are limited. For the dehydrogenated molecule, a small variation of the vdW energy at the interface is observed ( $-0.78 \pm 0.06$  eV), explained by the fact that this species presents the same adsorption topology independently of the coverage. The vdW energy between the molecules in the organic layer shows a limited variation from  $\theta = 0.2$  to 0.5 (Fig. 5(c)). The energies are  $-0.34 \pm 0.04$  eV for 8HQ, the tautomer and the hydrogenated species and  $-0.28 \pm 0.01$  eV for the dehydrogenated molecule. For low coverages, the vdW interactions between the molecules are minimized due to the large distance between the molecules. At high coverages ( $\theta \geq 0.5$ ), the great number of molecules on the Al(111) surface reduces the distance between the molecules and hence increases the vdW interactions between them. For all the molecules, the vdW energies in the organic layer are  $-0.43 \pm 0.07$  eV and  $-0.67 \pm 0.08$  eV for  $\theta = 0.66$  and  $\theta = 1$ , respectively. The decrease of the contribution of the vdW energy at the interface, when  $\theta$  increases, is compensated for by the increase of the vdW contribution between the molecules in the layer, in particular at full coverage. Besides the formation of covalent bonds between the molecules and the Al(111) surface, these results underline a strong contribution of vdW forces in the adsorption process.

### 3.1.3 Charge transfers, dipole moments and work function changes

*Charge transfers.* As defined previously, the global charge variation  $\Delta Q_{\text{mol}}$  is calculated by the difference between the total number of electrons on the adsorbed molecules and that of the free species calculated in vacuum. Strong electronic transfers from the substrate to the adsorbates were determined. Once adsorbed on Al(111), the  $\chi$ ,  $\tau$ ,  $\eta$  and  $\delta$  molecules were negatively charged. Fig. 6 shows the global charge variation on the molecules as a function of the coverage  $\theta$ . Independently of the coverage, the global charge variations in the molecules are  $-0.84 \pm 0.11 e$ ,  $-1.18 \pm 0.09 e$ ,  $-1.40 \pm 0.07 e$  and  $-1.50 \pm 0.09 e$  for the hydrogenated, the dehydrogenated, the native 8HQ and the tautomer species, respectively. Table 3 presents the charge

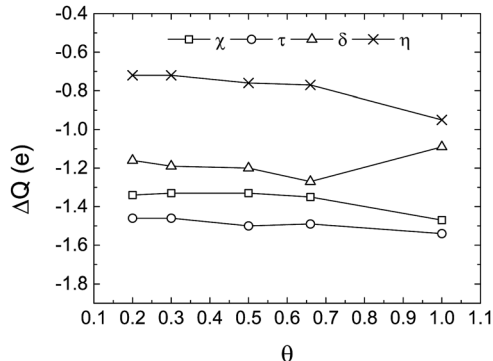


Fig. 6 Global charge variation as function of the coverage  $\theta$  of the 8HQ molecule and its derivatives after adsorption on the Al(111) surface. The 8HQ molecule ( $\chi$ ); the tautomer ( $\tau$ ); dehydrogenated 8HQ ( $\delta$ ); and hydrogenated 8HQ ( $\eta$ ).



**Table 3** Charge variation (in  $e$ ) of atoms as function of the coverage  $\theta$  after adsorption of the 8HQ molecule and its derivatives. Atoms X of the molecules bound to the Al atoms are also indicated Al(X)

	O	N	C2	C4	Al1(O)	Al2(N)	Al3(C2)	Al4(C4)
<b>8HQ</b>								
$\theta$ 0.2	-0.01	-0.25	-0.38	-0.24	+0.10	+0.66	+0.04	+0.56
$\theta$ 0.3	+0.03	-0.23	-0.29	-0.33	+0.08	+0.66	+0.03	+0.54
$\theta$ 0.5	-0.01	-0.26	-0.39	-0.32	+0.07	+0.66	+0.03	+0.55
$\theta$ 0.66	0.00	-0.26	-0.33	-0.32	+0.04	+0.66	+0.07	+0.57
$\theta$ 1	-0.09	-0.20	-0.78	+0.08	+0.41	+0.66	+0.55	-0.09
<b>Tautomer</b>								
$\theta$ 0.2	-0.16	-0.03	-0.19	-0.23	+0.73	+0.32	-0.01	+0.58
$\theta$ 0.3	-0.16	-0.05	-0.14	-0.25	+0.72	+0.30	+0.00	+0.58
$\theta$ 0.5	-0.17	-0.08	-0.23	-0.30	+0.71	+0.33	+0.00	+0.57
$\theta$ 0.66	-0.15	-0.07	-0.20	-0.29	+0.69	+0.31	-0.02	+0.58
$\theta$ 1	-0.19	-0.03	-0.58	+0.04	+0.75	+0.42	+0.58	-0.14
<b>Hydrogenated 8HQ</b>								
$\theta$ 0.2	-0.04	-0.08	-0.07	-0.33	+0.00	+0.34	-0.00	+0.59
$\theta$ 0.3	-0.08	-0.06	-0.03	-0.31	-0.01	+0.33	-0.01	+0.58
$\theta$ 0.5	-0.04	-0.07	+0.08	-0.34	-0.02	+0.31	-0.00	+0.58
$\theta$ 0.66	-0.08	-0.06	+0.05	-0.32	-0.05	+0.31	-0.02	+0.58
$\theta$ 1	-0.18	-0.06	-0.40	+0.01	+0.30	+0.35	+0.52	-0.12
<b>Dehydrogenated 8HQ</b>								
$\theta$ 0.2	-0.47	-0.17	-0.13	-0.19	+0.49	+0.89	-0.08	+0.00
$\theta$ 0.3	-0.47	-0.16	-0.17	-0.09	+0.48	+0.89	-0.08	-0.01
$\theta$ 0.5	-0.47	-0.15	-0.15	-0.24	+0.50	+0.88	-0.07	+0.00
$\theta$ 0.66	-0.47	-0.16	-0.17	-0.06	+0.50	+0.91	-0.04	-0.09
$\theta$ 1	-0.35	-0.13	-0.21	-0.17	+0.70	+0.55	-0.08	-0.06

variation on the atoms in the system due to the adsorption process. The net charge variation on the other atoms of the molecule and of the surface are negligible ( $\leq 0.01 e$ ). A detailed analysis of the values shows that the electron transfers are principally localized on the O, N, C2 and C4 atoms of the molecules and on the surface Al atoms. In the  $\tau$  and  $\eta$  molecules, the gains of electrons on the N atom (with the presence of a H-N bond) are lower than in  $\chi$  and  $\delta$  (nearly two times lower in  $\eta$  than in  $\chi$ ). Similarly, due to the presence of the H atom attached on the O atom of the hydroxyl group, the gains of electrons on the O atom in  $\chi$  and  $\eta$  are also lower than in  $\tau$  and  $\delta$ .

**Dipole moments.** In their free state, the 8HQ molecule and its derivatives are polar molecules, with an intrinsic dipole moment localized in the plane of the molecules and oriented from the oxygen atom to the electropositive area. The calculated dipole moment (in plane) of native 8HQ and the tautomer in vacuum are 2.5 D and 5.67 D respectively. Both forms can coexist in neutral solvents. We also modeled the 8HQ molecule in acidic and basic solutions using its hydrogenated and dehydrogenated forms. The dipole moments of these species in their free state are 1.92 D and 5.71 D for the  $\eta$  and  $\delta$  species respectively. In all these free molecules, the out of plane component of the dipole moment is zero. During the adsorption process, the electronic transfers induce the formation of a dipole at the molecule/metal interface. Fig. 7(a) presents the variation of the total dipole moment  $\mu_z(\text{mol/slab})$  normal to the surface for the molecule/metal systems as a function of the surface coverage  $\theta$  for the four molecules. The negative sign

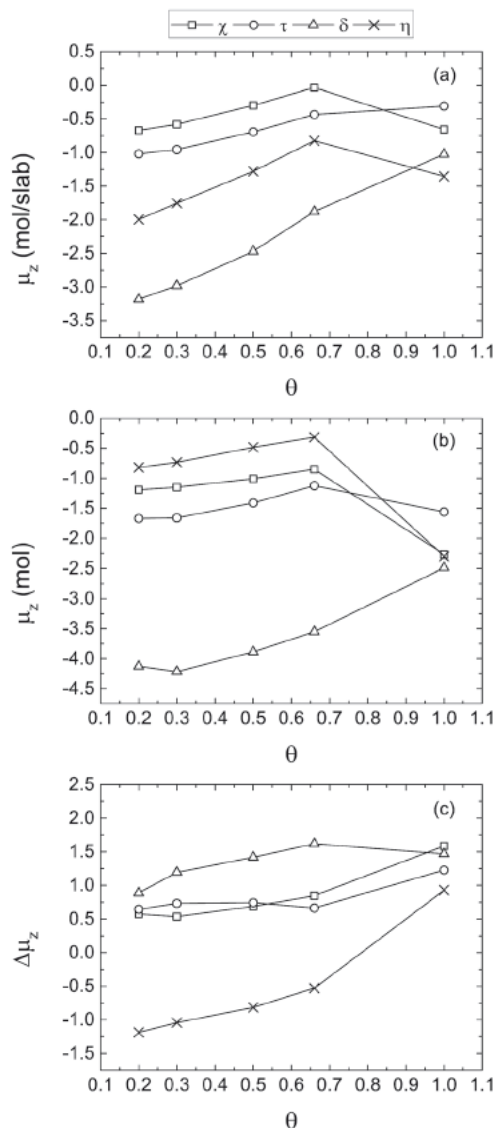


**Fig. 7** Dipole moments for different surface coverages  $\theta$ . (a):  $\mu_z(\text{mol/slab})$ ; (b):  $\mu_z(\text{mol})$ ; and (c):  $\Delta\mu_z$ . The 8HQ molecule ( $\chi$ ); dehydrogenated 8HQ ( $\delta$ ); and hydrogenated 8HQ ( $\eta$ ).

of  $\mu_z(\text{mol/slab})$  indicates that the dipole moment is oriented down to the Al(111) surface. The radical species (hydrogenated and dehydrogenated forms) induce higher dipole moments (in absolute value) than native 8HQ and the tautomer molecules. For all the species, the dipole moment  $\mu_z(\text{mol/slab})$  strength decreases linearly with increasing coverage up to  $\theta = 0.66$ . For  $\theta = 1$ , in the case of the native 8HQ molecule, the tautomer and the hydrogenated forms, there is a change in the molecular layer structure on Al(111) and in the electronic transfers that modifies  $\mu_z(\text{mol/slab})$ . For the dehydrogenated form, no change in the layer structure at high coverage is observed and the dipole moment still follows a linear decrease (in absolute value).

For a more detailed analysis,  $\mu_z(\text{mol/slab})$  can be decomposed into three contributions:

$$\mu_z(\text{mol/slab}) = \mu_z(\text{mol}) + \mu_z(\text{slab}) + \Delta\mu_z$$

where  $\mu_z(\text{mol})$  and  $\mu_z(\text{slab})$  are the components in the direction normal to the surface of the dipole moments for the molecular layer and the substrate at their geometry after adsorption, respectively. Thus  $\Delta\mu_z$  is the dipole moment induced at the interface by the electronic redistribution due to chemical interactions between the molecules and the substrate. This decomposition of  $\mu_z(\text{mol/slab})$  is artificial because all the components are closely linked. However, analyzing the variation of each component gives insight in the origin of the work function changes that we describe below.

Fig. 7(b) and (c) show the variation of  $\mu_z(\text{mol})$  and  $\Delta\mu_z$  as a function of the coverage  $\theta$  for all the adsorbed species on the Al(111) surface. The change of these two quantities can be attributed to the deformation and/or the orientation of the molecule which depend on the density of the molecular layer. The molecular dipolar component  $\mu_z(\text{mol})$  is oriented from the molecule down to the substrate and it has the same sign and the same decreasing trend with the coverage as  $\mu_z(\text{mol/slab})$ . However, the component induced by the charge transfer  $\Delta\mu_z$  is oriented oppositely (from the surface to the molecule,  $\Delta\mu_z$ ) to  $\mu_z(\text{mol})$ , except for the hydrogenated molecule  $\eta$  (see Fig. 7(c)). For all the adsorbed molecules (native 8HQ and its derivatives) the value of  $\mu_z(\text{slab})$  varies from 0.01 D to 0.05 D. This is negligible when compared to  $\mu_z(\text{mol})$  and  $\Delta\mu_z$ . The global interface dipole moment  $\mu_z(\text{mol/slab})$  is thus an equilibrium between the contribution of the molecular layer and the contribution at the interface related to the charge transfer.

To conclude, the magnitude of the molecular permanent dipole ( $\mu_z(\text{mol})$ ) and the variation of the dipole moment at the interface ( $\Delta\mu_z$ ) induced by electronic transfers are significant in the adsorption of 8HQ and derivatives on Al(111). Similar conclusions were reported for the adsorption of the Al(8HQ)<sub>3</sub> complex on cobalt,<sup>16</sup> whereas the dipole moment was dominated only by the molecular dipole moment in the adsorption of the Al(8HQ)<sub>3</sub> complex on magnesium<sup>17</sup> and aluminum<sup>18,19</sup> surfaces.

**Work function changes.** The work function is one of the properties affected by electronic changes due to the adsorption

of organic molecules on metallic surfaces and the interface dipole plays a crucial role in the work function shift. In the present work, the work function was calculated from the difference between the Fermi energy ( $E_F$ ) and the asymptotic electrostatic potential energy ( $V_\infty$ ) in the middle of the vacuum of the simulation cell:

$$\phi = V_\infty - E_F.$$

The work function change during the adsorption process was given by:

$$\Delta\phi = \phi(\text{mol/slab}) - \phi(\text{slab})$$

where  $\phi(\text{mol/slab})$  and  $\phi(\text{slab})$  are the work function of the molecule/metal systems and the bare Al(111) surface, respectively.

Fig. 8(a) shows the work function variation as a function of the surface coverage  $\theta$ . Unlike the adsorption energy and the electronic transfers, which show a low dependence on the coverage  $\theta$ , the work function change is strongly sensitive to the adsorption topology of the molecules, which depends on the coverage. In all cases, the adsorption of the 8HQ molecule and its derivatives on the Al(111) surface reduces significantly the work function of the substrate ( $\Delta\phi \leq 0$ ) with a change of the work function between 0.1 and 1.4 eV. These values are in agreement with experimental work function changes (0.8 to 1.5 eV) and DFT computed values (0.9 to 1.7 eV) determined for the adsorption of the Al(8HQ)<sub>3</sub> complex on an aluminum surface.<sup>18,19</sup> The shift of the work function  $\Delta\phi$  as a function of  $\theta$  is attributed to the electron redistribution due to the molecules' chemisorption on Al(111) and to the charge transfers between the substrate and the adsorbates. Moreover, the polarization effects due to van der Waals forces change with the topology of the adsorbate and also modify the work function of the system. It is known as "the push back effect"<sup>23,44,45</sup> where the electron cloud of the metal is compressed by the electron cloud of the adsorbed molecule.

For  $\theta = 0.2$  to 0.66, the dehydrogenated species  $\delta$  shows the largest change of the work function followed by the hydrogenated

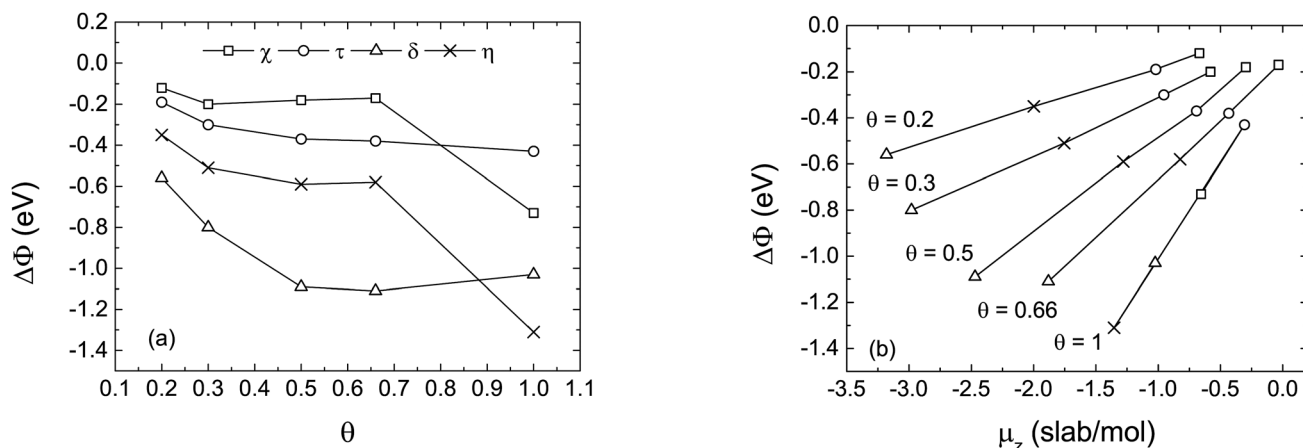


Fig. 8 Work function change ( $\Delta\phi$ ) as a function of the surface coverage and relationships between the work function change ( $\Delta\phi$ ) and the dipole moment ( $\mu_z(\text{slab/mol})$ ) at each coverage  $\theta$ . The 8HQ molecule ( $\chi$ ); the tautomer ( $\tau$ ); dehydrogenated 8HQ ( $\delta$ ); and hydrogenated 8HQ ( $\eta$ ).

species  $\eta$ , the tautomer  $\tau$  and finally the native 8HQ molecule  $\chi(\Delta\phi(\delta) \leq \Delta\phi(\eta) \leq \Delta\phi(\tau) \leq \Delta\phi(\chi))$ . It is not possible to find any correlation between the total electronic transfer from the substrate to the adsorbed molecules and the work function changes because of different adsorption geometries of  $\chi, \tau, \eta$  and  $\delta$  species.

For  $\theta = 1$ , a different order in the ranking of the work function change induced by the adsorbed molecules is observed and the largest work function change is for the tautomer/Al(111) system ( $\Delta\phi(\eta) \leq \Delta\phi(\delta) \leq \Delta\phi(\chi) \leq \Delta\phi(\tau)$ ). In that case where all the molecules have similar adsorption geometries, the work function variation varies as the reverse of the total electronic transfer ( $\Delta Q_{\text{mol}} = -0.95, -1.10, -1.47, -1.54 e$  for  $\eta, \delta, \chi$  and  $\tau$  respectively). To conclude, the work function change depends on the nature of the adsorbate and on the coverage.

The relation between the work function variation and the interface dipole moment  $\mu_z(\text{mol/slab})$  was also investigated. Fig. 8(b) presents the work function change  $\Delta\phi$  as a function of  $\mu_z(\text{mol/slab})$  at different coverages (from  $\theta = 0.2$  to 1). The correlation between the work function variation and the interface dipole moment  $\mu_z(\text{mol/slab})$  follows a linear variation as proposed by the Helmholtz model:  $\Delta\phi = -4\pi\theta\mu_z$  (in atomic units), with the slope of the lines increasing with  $\theta$ .

### 3.2 Adsorption of molecular oxygen on the protected Al(111) surface

In order to verify the efficiency of these protective layers against oxygen reduction which is the cathodic reaction involved in the corrosion process, the interaction of molecular oxygen with the covered Al(111) surface was also investigated for two surface coverages: (i)  $\theta = 0.66$  where the Al surface is totally covered by molecules parallel to the surface for the 8HQ and tautomer species and by molecules tilted on the surface in the case of the dehydrogenated form, and (ii)  $\theta = 1$  where all the organic species are tilted on the metallic surface. The interaction of  $\text{O}_2$  on the Al(111) surface covered with the hydrogenated species was not studied because it will be shown in the following that the presence of a hydroxyl  $-\text{OH}$  or an amino  $-\text{NH}$  chemical group on the organic molecule favors the dissociation of the  $\text{O}_2$  molecule.

For  $\theta = 0.66$ , the main results concerning the geometrical changes in the layer ( $\chi, \tau$  or  $\delta$  species) due to interactions with  $\text{O}_2$  are presented in Table 4. For the native 8HQ molecule, a spontaneous dissociation of the  $\text{O}_2$  molecule is obtained when it is positioned on top of the N atom of the adsorbed molecule. The resulting geometry is shown in Fig. 9(a). In the free  $\text{O}_2$  molecule, the calculated O–O distance is 1.23 Å. After the adsorption on the partially 8HQ-covered surface ( $\theta = 0.66$ ), the O–O distance is increased to 2.83 Å. In fact, one of the O atoms ( $\text{O}_a$ ), initially placed at more than 2 Å from the hydroxyl group of the 8HQ molecule, captures the H atom of this group with a final  $\text{O}_a$ –H distance of 0.98 Å. This atom ( $\text{O}_a$ ) is adsorbed on-top of an Al atom with a distance  $\text{O}_a$ –Al of 1.76 Å. The second O atom ( $\text{O}_b$ ) is adsorbed on a threefold symmetry site (hcp) of the surface not covered by the molecules with an averaged  $\text{O}_b$ –Al distance of 1.84 Å. Due to this reaction, the native 8HQ molecule becomes dehydrogenated by losing the H atom of the hydroxyl group (Fig. 9) and adopts a geometry with three covalent bonds (between O, N, C4 atoms and Al atoms) similar to the adsorption geometry of  $\delta$  at low coverage<sup>20</sup> (presented in Table 4 as  $\delta_2$ ). The net charges of the  $\text{O}_a$  and  $\text{O}_b$  atoms after the dissociation of the  $\text{O}_a$ – $\text{O}_b$  molecule are respectively  $-1.52 e$  and  $-1.73 e$ . Finally, the total energy variation in the system during the  $\text{O}_2$  reduction process is  $-8.16 eV$ . This value was calculated as the difference between the total energy of the system after  $\text{O}_2$  adsorption and the sum of the total energy of the 8HQ/Al(111) system and the free  $\text{O}_2$  molecule.

The interaction of the  $\text{O}_2$  molecule on the Al(111) surface covered by the tautomer  $\tau$  for  $\theta = 0.66$  is similar to the case of  $\chi$  with a lower total energy variation ( $-7.19 eV$ ). The final geometry is shown in Fig. 9. After the dissociation, the  $\text{O}_a$ – $\text{O}_b$  distance is 2.81 Å. One of the O atoms ( $\text{O}_a$ ) has taken the H atom of the NH group of the tautomer and is adsorbed on top of an Al atom in the Al(111) surface with an  $\text{O}_a$ –Al distance of 1.75 Å. The length of the  $\text{O}_a$ –H bond is 0.98 Å. The second O atom ( $\text{O}_b$ ) of the oxygen molecule is adsorbed on a hcp site of the Al(111) surface with an average  $\text{O}_b$ –Al distance of 1.84 Å. One of the four tautomer molecules in the simulation cell is thus dehydrogenated during the  $\text{O}_2$  reduction. Again, the bond

**Table 4** Geometrical parameters of the molecules in the native 8HQ, tautomer and dehydrogenated layers adsorbed on Al(111) for a coverage  $\theta = 0.66$  before and after reduction of an  $\text{O}_2$  molecule

	$d_{\text{C}2\text{C}3}$	$d_{\text{C}3\text{C}4}$	$d_{\text{C}4\text{C}10}$	$d_{\text{C}10\text{C}5}$	$d_{\text{C}5\text{C}6}$	$d_{\text{C}6\text{C}7}$	$d_{\text{C}7\text{C}8}$	$d_{\text{C}8\text{C}9}$	$d_{\text{C}9\text{C}10}$	$d_{\text{C}9\text{N}}$	$d_{\text{C}2\text{N}}$	$d_{\text{C}8\text{O}}$	$d_{\text{OH}}$	$d_{\text{NH}}$
<b>8HQ</b>														
Free mol.	1.417	1.381	1.418	1.419	1.383	1.415	1.385	1.431	1.430	1.361	1.325	1.355	0.990	2.051
$\theta = 0.66$	1.368	1.472	1.476	1.405	1.401	1.400	1.399	1.408	1.413	1.419	1.415	1.375	0.990	2.140
$\theta = 0.66 + \text{O}_2$	1.366	1.470	1.477	1.402	1.401	1.396	1.412	1.425	1.421	1.415	1.401	1.348	2.222	2.300
<b>Tauto</b>														
Free mol.	1.404	1.388	1.421	1.406	1.402	1.401	1.426	1.466	1.434	1.350	1.338	1.270	2.064	1.041
$\theta = 0.66$	1.352	1.472	1.480	1.406	1.399	1.399	1.408	1.411	1.406	1.442	1.439	1.352	2.354	1.026
$\theta = 0.66 + \text{O}_2$	1.366	1.471	1.479	1.402	1.401	1.397	1.410	1.423	1.422	1.410	1.408	1.355	1.936	2.722
<b>Deh. 8HQ</b>														
Free mol.	1.410	1.384	1.414	1.426	1.399	1.387	1.456	1.496	1.431	1.344	1.334	1.249		
$\delta_2^{20}$	1.368	1.465	1.475	1.403	1.401	1.397	1.413	1.425	1.421	1.408	1.406	1.346		
$\theta = 0.66$	1.401	1.390	1.420	1.419	1.389	1.412	1.390	1.417	1.425	1.375	1.349	1.366		
$\theta = 0.66 + \text{O}_2$	1.401	1.390	1.420	1.418	1.388	1.412	1.388	1.414	1.425	1.375	1.348	1.365		

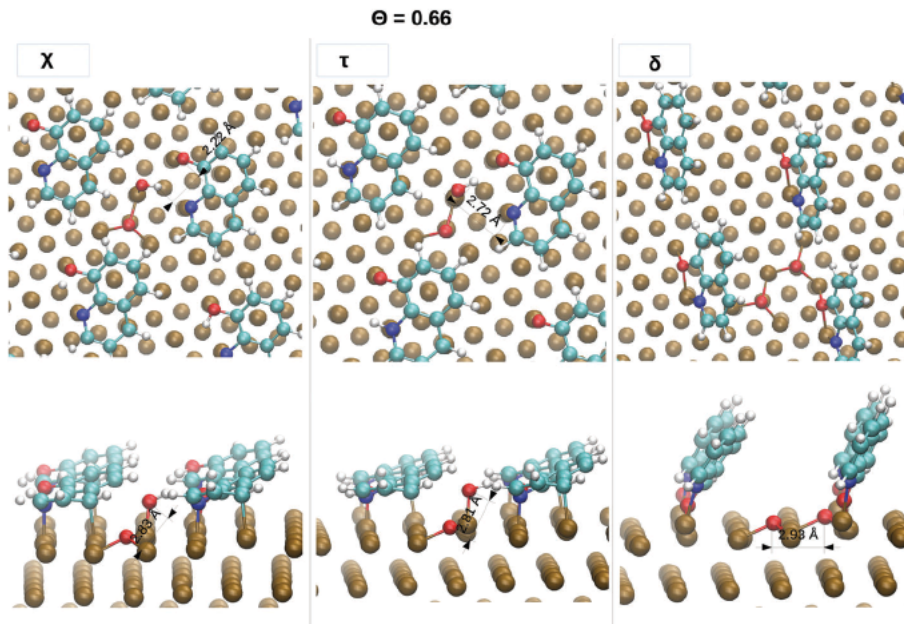


Fig. 9  $O_2$  interaction with the Al(111) surface covered ( $\theta = 0.66$ ) by: (a): a native 8HQ layer; (b): a tautomer layer; and (c): a dehydrogenated 8HQ layer.  $O_a$  and  $O_b$  are the atoms of the initial  $O_2$  molecule. The dark blue and the black arrow represent the  $O_a$ -H and the  $O_a$ - $O_b$  distances, respectively.

lengths and distances in the 'dehydrogenated tautomer' molecule after the adsorption of  $O_2$  are similar to those of one adsorbed mode of the dehydrogenated species determined previously at low coverage<sup>20</sup> and also presented in Table 4 (the  $\delta_2$  mode for  $\theta = 0.2$ ). After dissociation, the net charges on the  $O_a$  and  $O_b$  atoms are  $-1.42 e$  and  $-1.72 e$ , respectively, similar to the case of the adsorption of  $O_2$  in the presence of the native 8HQ molecule. In both cases, the surface Al atoms give electrons to the  $O_2$  molecule and are thus oxidized.

The difference between the energy variations during the  $O_2$  reduction on Al(111) in the presence of 8HQ or the tautomer layer is 1 eV. During the reduction process, there is an uptake of one H atom by the  $O_2$  molecule. This leads to the dehydrogenation of one inhibitor molecule ( $\chi$  or  $\tau$ ) and the geometrical relaxation on Al(111) of the molecule that is dehydrogenated. The energy released by this geometrical relaxation is different in each case because the initial geometries are different (one is the geometry of 8HQ on Al(111) and the other one is the geometry of the tautomer on Al(111)) and the difference between the adsorption energy of 8HQ and the adsorption energy of the tautomer molecules on Al(111) is 1 eV. The energetic difference of 1 eV between the  $O_2$  reduction processes on the 8HQ and tautomer layers is thus mainly due to the dehydrogenation and geometrical relaxation of the dehydrogenated  $\chi$  or  $\tau$  inhibitor molecules.

We have demonstrated above that the dehydrogenated 8HQ molecule is the most stable layer on Al(111) with a topology of the molecules tilted on the metallic surface. For  $\theta = 0.66$ , there is still some surface area not protected by the molecules.  $O_2$  dissociation occurs on the Al(111) surface (see Fig. 9) with an energy variation of  $-8.86$  eV (taking as references the  $O_2$  free molecule and the metallic slab covered by the dehydrogenated

molecules for  $\theta = 0.66$ ) and a final  $O_a$ - $O_b$  distance of 2.93 Å. The  $O_a$  and  $O_b$  atoms are adsorbed in hcp sites on the Al(111) surface and there is an electronic transfer from the Al atoms to the  $O_a$  and  $O_b$  atoms (electronic gains of 1.74  $e$  on each  $O_a$  and  $O_b$  atoms). The dehydrogenated molecules are only slightly affected by the electronic transfers and no geometrical changes in the organic layer are observed during the  $O_2$  reduction (see bond lengths in Table 4).

At a higher coverage ( $\theta = 1$ ), as shown in Fig. 2, for all the 8HQ species (native 8HQ, the tautomer, and the dehydrogenated molecules), the Al(111) surface is totally covered. The  $O_2$  molecule does not interact or is only physisorbed on the molecular layer in all the cases with no change in the O-O distance in the  $O_2$  molecule, kept at the bond length of the free  $O_2$  molecule. There is no electronic transfer to the  $O_2$  molecule and the organic layer thus forms an efficient barrier against electronic transfer from the Al substrate to the  $O_2$  molecule.

## 4 Conclusions

In the present work, the interaction of 8HQ molecules and derivatives with the Al(111) surface is investigated from low to high coverage. For  $\theta = 0.2$  to 1, the calculations were performed in the framework of dispersion corrected Density Functional Theory (DFT-D). For all the molecules studied, stable chemisorbed configurations are determined with the formation of covalent bonds between the organic molecules and the metal surface and a significant contribution of vdW interactions. These latter interactions are especially strong at the molecule/metal interface at low coverage and between the molecules in the organic layers at high coverage. During the chemisorption

process, the molecules are strongly deformed, which reduces the adsorption energies. Among the 8HQ molecule and its derivatives, the dehydrogenated species has the strongest coupling with the Al(111) surface and adopts similar adsorption topologies independently of the coverage. In contrast, the native 8HQ, tautomer and hydrogenated species exhibit a structural change in their adsorption topologies between low and high coverage. The strongest bonding on Al(111) of the dehydrogenated species, present in alkaline aqueous solutions, is in agreement with recent experimental results (electrochemical measurements and surface analysis) showing that the 8HQ molecule is especially efficient in alkaline solutions (these results are unpublished because studies are still in progress).

For all the coverages and all the adsorbed species, localized electronic transfers from the substrate to the adsorbates are observed. The electronic density redistribution due to the adsorption of the molecules induces the reduction of the work function of the metal. The increase of the coverage leads to the strongest change of the work function. This variation is linked to the formation of a dipole at the molecule/metal interface and of a dipole in the organic layer.

To demonstrate that the formation of a complete layer of 8HQ molecules or derivatives on Al(111) can inhibit aluminum corrosion, molecular oxygen reduction on the covered aluminum surface is also investigated. This reaction is one of the elementary reactions occurring during the corrosion process of aluminum. At low coverage, dissociation of the O<sub>2</sub> molecule occurs on uncovered areas of the Al(111) surface. At full coverage ( $\theta = 1$ ), O<sub>2</sub> dissociation does not happen in the presence of the organic layers thus preventing aluminum atoms from further oxidation (no electronic transfer). 8HQ layers on Al(111) form a protective barrier against corrosion of the Al substrate.

## Conflicts of interest

There are no conflicts to declare.

## Acknowledgements

This work was performed using HPC resources from CALMIP (Grant p12174) and from CINES (Grant c2013097076). It was supported by the National Research Agency (ANR number ANR-2011 JS08 015 01). The authors thank Nathalie Tarrat from CEMES, Toulouse, for very fruitful discussions.

## References

- 1 P. Raja and M. Sethuraman, *Mater. Lett.*, 2008, **62**, 113–116.
- 2 G. Gece, *Corros. Sci.*, 2011, **53**, 3873–3896.
- 3 D. Costa and P. Marcus, *Molecular Modeling of Corrosion Processes: Scientific Development and Engineering Applications*, John Wiley & Sons, Inc, Hoboken, 2015, ch. 5.
- 4 L. Garrigues, N. Pèbère and F. Dabosi, *Electrochim. Acta*, 1996, **41**, 1209–1215.
- 5 C. Casenave, N. Pèbère and F. Dabosi, *Mater. Sci. Forum*, 1995, 599–610.
- 6 S. V. Lamaka, M. L. Zheludkevich, K. A. Yasakau, M. F. Montemor and M. G. S. Ferreira, *Electrochim. Acta*, 2007, **52**, 7231–7247.
- 7 L. Song-mei, Z. Hong-rui and L. Jian-hua, *Trans. Nonferrous Met. Soc. China*, 2007, **17**, 318–325.
- 8 A. S. Yaro and H. A. Dahyool, *Iraqi Journal of Chemical and Petroleum Engineering*, 2009, **10**, 19–25.
- 9 H. N. Soliman, *Corros. Sci.*, 2011, **53**, 2994–3006.
- 10 K. A. Yasakau, M. L. Zheludkevich, O. V. Karavai and M. G. S. Ferreira, *Prog. Org. Coat.*, 2008, **63**, 352–361.
- 11 A. C. Balaskas, I. A. Kartsonakis, L.-A. Tziveleka and G. C. Kordas, *Prog. Org. Coat.*, 2012, **74**, 418–426.
- 12 Z. Tian, H. Shi, F. Liu, S. Xu and E.-H. Han, *Prog. Org. Coat.*, 2015, **82**, 81–90.
- 13 A. C. Balaskas, M. Curioni and G. E. Thompson, *Surf. Interface Anal.*, 2015, **47**, 1029–1039.
- 14 S. Marcelin and N. Pèbère, *Corros. Sci.*, 2015, **101**, 66–74.
- 15 J. Zhang, P. Chen, B. Yuan, W. Ji, Z. Cheng and X. Qiu, *Science*, 2013, **342**, 611–614.
- 16 Y.-P. Wang, X.-F. Han, Y.-N. Wu and H.-P. Cheng, *Phys. Rev. B: Condens. Matter Mater. Phys.*, 2012, **85**, 144430.
- 17 S. Yanagisawa and Y. Morikawa, *J. Phys.: Condens. Matter*, 2009, **21**, 064247.
- 18 S. Yanagisawa and Y. Morikawa, *Chem. Phys. Lett.*, 2006, **420**, 523–528.
- 19 S. Yanagisawa, K. Lee and Y. Morikawa, *J. Chem. Phys.*, 2008, **128**, 244704.
- 20 F. Chiter, C. Lacaze-Dufaure, H. Tang and N. Pèbère, *Phys. Chem. Chem. Phys.*, 2015, **17**, 22243.
- 21 A. Kokalj, *Faraday Discuss.*, 2015, **180**, 415.
- 22 Y. Jiang and J. B. Adams, *Surf. Sci.*, 2003, **529**, 428–442.
- 23 A. Kokalj, S. Peljhan, M. Finšgar and I. Milošev, *J. Am. Chem. Soc.*, 2010, **132**, 16657–16668.
- 24 Y. Jiang, J. B. Adams and D. Sun, *J. Phys. Chem. B*, 2004, **108**, 12851–12857.
- 25 C. Gattinoni and A. Michaelides, *Faraday Discuss.*, 2015, **180**, 439–458.
- 26 S. Irrera, D. Costa and P. Marcus, *J. Mol. Struct. THEOCHEM*, 2009, **903**, 49–58.
- 27 M. M. Islam, B. Diawara, P. Marcus and D. Costa, *Catal. Today*, 2011, **177**, 39–49.
- 28 G. Kresse and J. Hafner, *Phys. Rev. B: Condens. Matter Mater. Phys.*, 1993, **47**, 558–561.
- 29 G. Kresse and J. Furthmuller, *Phys. Rev. B: Condens. Matter Mater. Phys.*, 1996, **54**, 11169–11186.
- 30 G. Kresse and J. Furthmuller, *Comput. Mater. Sci.*, 1996, **6**, 15–50.
- 31 P. E. Blochl, *Phys. Rev. B: Condens. Matter Mater. Phys.*, 1994, **50**, 17953–17979.
- 32 G. Kresse and D. Joubert, *Phys. Rev. B: Condens. Matter Mater. Phys.*, 1999, **59**, 1758–1775.
- 33 J. P. Perdew, K. Burke and M. Ernzerhof, *Phys. Rev. Lett.*, 1996, **77**, 3835.
- 34 J. P. Perdew, K. Burke and M. Ernzerhof, *Phys. Rev. Lett.*, 1997, **78**, 1396.

- 35 M. Methfessel and A. T. Paxton, *Phys. Rev. B: Condens. Matter Mater. Phys.*, 1989, **40**, 3616.
- 36 H. J. Monkhorst and J. D. Pack, *Phys. Rev. B: Condens. Matter Mater. Phys.*, 1976, **13**, 5188.
- 37 S. Grimme, *J. Comput. Chem.*, 2006, **27**, 1787.
- 38 W. Tang, E. Sanville and G. Henkelman, *J. Phys.: Condens. Matter*, 2009, **21**, 084204.
- 39 P. Roychowdhury, B. N. Das and B. S. Basak, *Acta Crystallogr., Sect. B: Struct. Crystallogr. Cryst. Chem.*, 1978, **34**, 1047–1048.
- 40 E. Bardez, I. Devol, B. Larrey and B. Valeur, *J. Phys. Chem. B*, 1997, **101**, 7786–7793.
- 41 M. Amati, S. Belviso, P. Cristinziano, C. Minichino, F. Lelj, I. Aiello, M. L. Deda and M. Ghedini, *J. Phys. Chem. A*, 2007, **111**, 13403–13414.
- 42 E. M. Filip, I. V. Humelnicu and C. I. Ghirvu, *Acta Chem. Iasi*, 2009, **17**, 85–96.
- 43 N. Kovačević and A. Kokalj, *Mater. Chem. Phys.*, 2012, **137**, 331–339.
- 44 G. Heimel, L. Romaner, E. Zojet and J. Bredas, *Acc. Chem. Res.*, 2008, **41**, 721–729.
- 45 B. J. Topham, M. Kumar and Z. G. Soos, *Adv. Funct. Mater.*, 2011, **21**, 1931.

# Electronic Supplementary Information (ESI)

## Corrosion protection of Al(111) by 8-hydroxyquinoline: a comprehensive DFT study

### Dimer adsorption

We tested additional initial geometries including the adsorption of dimer assemblies of 8HQ molecules. The optimized geometries are presented in Figure 1.

We calculated the total adsorption energy of the dimer, the adsorption energy per 8HQ molecule and the binding energy.

$$E_{ads/dimer} = E_{slab+dimer} - E_{slab/opt} - E_{freedimer/opt} \quad (1)$$

$$E_{ads/8HQmolecule} = E_{ads/dimer}/2 \quad (2)$$

$$E_{bind/8HQmolecule} = E_{slab+dimer} - E_{slab/sp} - E_{dimer-layer/sp} \quad (3)$$

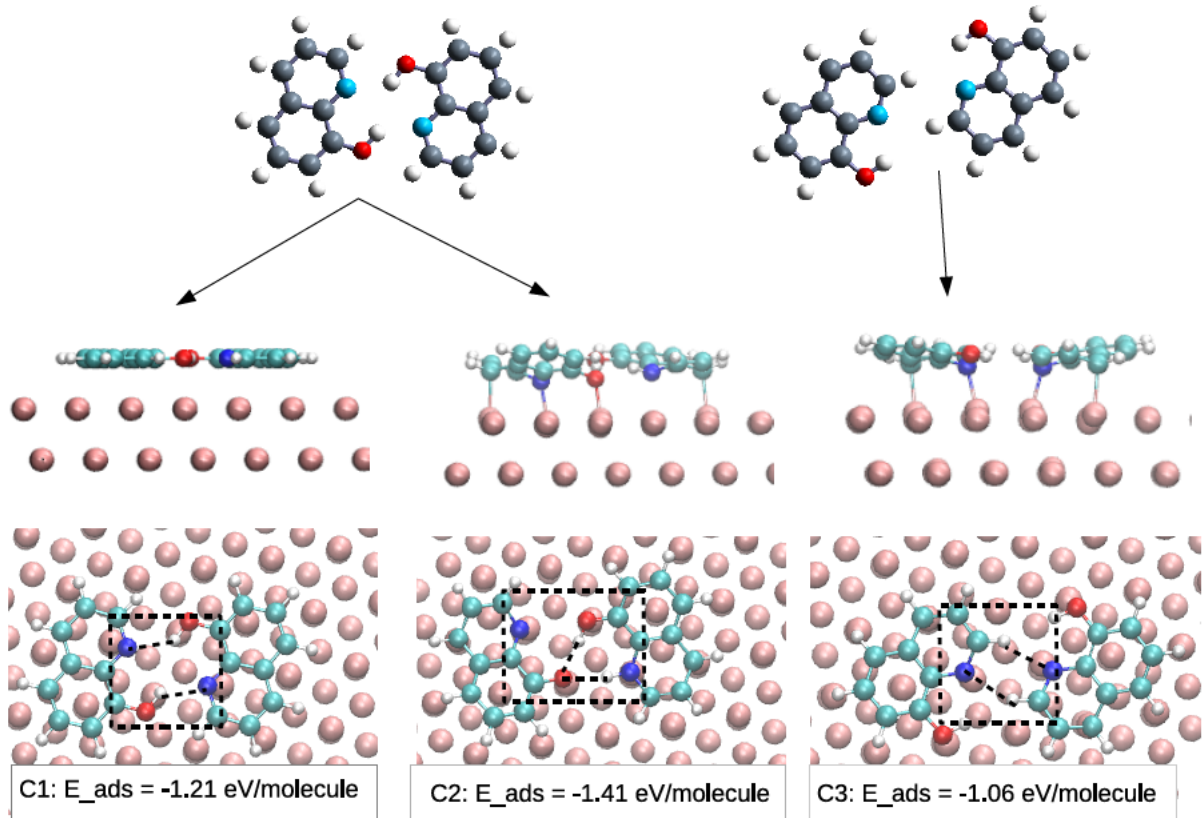


Figure 1: Adsorption topologies of dimer assemblies of 8HQ molecules on Al(111)Left: conformation C1. Middle: conformation C2. Right: conformationC3.

Where  $E_{slab+dimer}$  is the total energy of the system with the dimer molecule adsorbed on the Al(111) surface,  $E_{slab/opt}$  is the energy of the bare relaxed Al(111) slab calculated without dispersive corrections and  $E_{freedimer/opt}$  is the energy of the free dimer optimized in vacuum,  $E_{slab/sp}$  and  $E_{dimer-layer/sp}$  are the total energies of the isolated slab and isolated deformed dimer layer at their geometry after adsorption, respectively.

The results are presented in Table 1.  $\chi$  8HQ monomer corresponds to the native 8HQ molecule,  $\delta$  8HQ monomer to the dehydrogenated species and  $\eta$  8HQ monomer to the hydrogenated species.

We observed the formation of different H-bonding in the dimer (-OH...N, -OH...O, -NH...O, -CH...N). A physisorbed mode was found (see Figure 1 (C1)). In that case the total adsorption energy  $E_{ads/dimer}$  was -2.42 eV for the dimer (taking as the reference the free dimer species) or -1.21 eV/8HQmolecule. The adsorbed dimer geometry is not modified when compared to the free dimer species and  $E_{bind/8HQmolecule}$ , the binding energy per 8HQ molecule on the Al(111) surface, has a value of -1.21 eV. The 8HQ monomer binds



Table 1: H bond length in Å between the atoms of the 8HQ dimer assemblies after adsorption on Al(111), adsorption and binding energies in eV.

Conformations	H bond length	$E_{ads/dimer}$	$E_{ads/8HQmolecule}$	$E_{bind/8HQmolecule}$
C1 on Al(111)	OH N: 1.99	-2.42	-1.21	-1.21
C2 on Al(111)	OH O: 1.78	-2.82	-1.41	/
	NH O: 1.95			
C3 on Al(111)	CH N: 2.33	-2.12	-1.06	-2.88
$\chi$ 8HQ monomer on Al(111)	/	/	-1.11	-2.90
$\delta$ 8HQ monomer on Al(111)	/	/	-3.44	-4.20
$\eta$ 8HQ monomer on Al(111)	/	/	-1.71	-2.31

stronger to the surface than in the case of the dimer (Binding energy: -2.90 eV/molecule for the 8HQ monomer and -1.21 eV/8HQmolecule when the 8HQ is in the form of the dimer). Others conformations are chemisorbed conformations with the formation of covalent bonds between the molecules and the Al surface atoms. It indicates the strong affinity of the 8HQ molecule with aluminum. Two conformations are shown in Figure 1 (C2) and (C3). The most stable adsorption topology of the dimer on the Al(111) surface led to a chemical modification of the organic species (Figure 1 (C2)): one H atom of the hydroxyl group of one 8HQ molecule is transferred to the other 8HQ molecule. The 8HQ dimer becomes thus one hydrogenated and one dehydrogenated species on Al(111) with conformations of the two molecules on the Al(111) surface similar to the conformation of the dehydrogenated  $\delta$  and hydrogenated  $\eta$  monomers at low coverage (see Table 1 and also presented in the manuscript) but with H bonding between the two species. The total adsorption energy is -2.82 eV (taking as the reference the free dimer species) or -1.41 eV/molecule if we divide the latter value by the number of monomers in the dimer. In our manuscript, for the adsorption of the monomer species, i.e. adsorption of only one type of species for each calculation, the adsorption energy of the dehydrogenated  $\delta$  molecules is -3.44 eV/molecule independently of the coverage and the adsorption energy of the hydrogenated species is -1.71 eV/molecule independently of the coverage. So the binding of only one type of species is stronger than the adsorption energy of the same species in the modified dimer (averaged at -1.41 eV per molecule). For the conformation in Figure 1 (C3), the total adsorption energy is -2.12 eV for the dimer (taking as the reference the free dimer species) and then -1.06 eV/molecule, and the binding energy per 8HQ

monomer on the Al(111) is -2.88 eV/molecule. The geometries of the 8HQ molecules in the adsorbed dimer species are the same as the geometry of one 8HQ monomer adsorbed on Al(111). In the work presented in the revised manuscript, the adsorption energy for one 8HQ monomer is about -1.11 eV/molecule independently of the surface coverage. The 8HQ monomer binds slightly stronger to the surface than in the case of the dimer (Binding energy: -2.90 eV/molecule for the 8HQ monomer and -2.88 eV/8HQmolecule when the 8HQ is in the form of the dimer). These results show that the association of the molecules as dimers on the Al(111) surface is thus not favored over the adsorption of monomer species, presented in the article.